KINEMATIC FIELD OF THE S-SHAPED NEBULA N119 IN THE LMC[1]

P. Ambrocio-Cruz,[2,5] M. Rosado,[2] A. Laval,[4] E. Le Coarer,[3] D. Russeil,[4] and P. Amram[4]

RESUMEN

La nebulosa N119 en la Nube Mayor de Magallanes tiene una morfología muy peculiar, difícil de explicar con los modelos clásicos. El objetivo del presente artículo es proporcionar datos cinemáticos que puedan dar restricciones sobre su naturaleza, formación y evolución. La peculiar morfología espiral de esta nebulosa se ve reflejada en su campo de velocidades radiales, el cual muestra varias expansiones en los filamentos débiles, los cuales forman diferentes regiones en forma de burbujas, pero también encontramos otras componentes cuyo origen no está claro. De acuerdo con nuestros resultados, N119 parece contener 3 nebulosas en forma de burbuja formadas por los vientos estelares de estrellas O, WR y quizás un posible remanente de una explosión de hipernova. En el curso de este estudio hemos detectado por primera vez una burbuja alrededor de la estrella WR Br 21.

ABSTRACT

The nebula N119 in the Large Magellanic Cloud shows a very conspicuous morphology difficult to explain with classical models. The aim of the present paper is to provide kinematic data that could place constraints on the nature, formation and evolution of N119. The peculiar spiral shape of this nebula is also reflected in a peculiar radial velocity field, showing several expansions of the faint filaments which form different bubble-like regions, and another component whose origin remains unrevealed. N119 seems to contain three expanding bubble-shaped nebulae formed by the action of the stellar winds from Wolf-Rayet and O stars, and a possible remnant of an hypernova explosion. Indeed, we have detected for the first time a bubble around the WR star Br 21, inside the N119 nebula.

Key Words: H II regions — ISM: bubbles — ISM: individual (N 119) — ISM: kinematics and dynamics — ISM: supernova remnants

1. GENERAL

Photoionizing radiation, stellar winds and supernova explosions from massive stars transform the interstellar medium (ISM) of a galaxy into a medium mainly formed by ionized bubbles filled with hot gas. Bubble and superbubble formation is generally attributed to stellar winds, and supernova explosions of massive stars. Induced star formation can explain the morphology of bubble-like nebulae and rings having HII regions at their boundaries, but other morphologies are difficult to explain.

In the Large Magellanic Cloud (LMC) there is a plethora of ring-shaped nebulae whose origins can be explained by one of the mechanisms mentioned above (Georgelin et al. 1983; Meaburn, Mc Gee, & Newton 1984; Rosado 1986). However, the nebula N 119 shows a very conspicuous form, difficult to explain with the classical events that could give rise to bubble formation. Indeed, this nebula shows a spiral morphology which still remains an enigma. It is also important to note the location of this weird nebula in the LMC. The nebula N 119 ($\alpha = 05^h 18.4^m, \delta = -69°15'$ in J2000 equinox) is located very close ($\sim 15'$ to the southeast) to the center of rotation of the disk of the LMC (Kim et al. 1998) and is seen projected in front of the bar of the LMC.

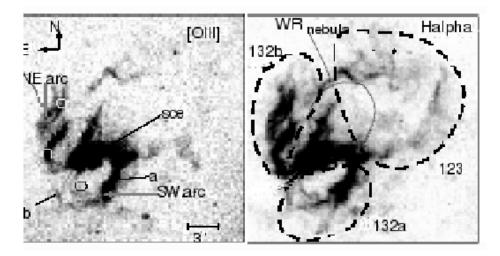The aim of the present paper is to provide kinematic data that could place constraints on the na-

Fig. 1. Monochromatic images of the field around N 119. The scale is the same for each map. (a) [OIII] emission and (b) Hα emission. In Panel (a) the position of the CO clouds is shown by circles; label *sce* shows the strong central emission, *a* shows the bright and broad arc and *b* shows the faint east filament. The bubble DEM L123 and the nebulae DEM L132a,b and WR nebula are marked in Panel (b).

ture, formation and evolution of N 119. In the next section, we give information about the Fabry-Perot observations carried out in order to obtain the kinematics of N 119. In § 3 we present the main characteristics and the local environment of N 119. § 4 describes the velocity field of the nebula. § 5 is devoted to a discussion of the kinematic results. Finally, § 6 presents the conclusions of this work.

2. OBSERVATIONS AND DATA REDUCTION

The observations on N119 were carried out with a scanning Fabry-Perot (FP) interferometer attached to the Cassegrain focus of the 36 cm telescope of the European Southern Observatory at La Silla and operated under the same conditions as during the observations of the H II region N103 described in Ambrocio-Cruz et al. (1997). With a $38' \times 38'$ field of view, and an angular sampling resolution of the photon-counting detector used of $9''$, we have obtained 3D velocity cubes with this angular field and resolution. The free spectral range of the FP has been scanned in 24 different etalon spacing positions giving sampling spectral resolutions of 16 km s^{-1} for the Hα line and 7 km s^{-1} for the [O III] line, respectively. Consequently, the FP data cube sizes are 254 $\times$ 254 $\times$ 24.

We have obtained FP data cubes at Hα and [O III](λ5007 Å). The calibration data cubes were taken before and after the nebular exposures in order to check for possible flexures of the equipment. The nebular data cubes have total exposure times of 7200s and 8000s for Hα and [O III], respectively.
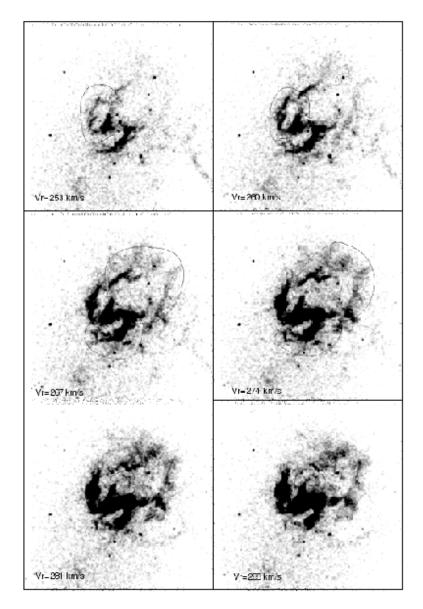
The data reduction was performed by means of the specialized software CIGALE (Le Coarer et al. 1993) which allows flat fielding correction, wavelength calibration, construction of the velocity maps and radial velocity profile extraction and fitting. Using this software we also were able to construct "monochromatic" and "continuum" images from the FP data cubes. The decomposition of profiles was constrained by adjusting the minumum number of components possible. Since we have good spatial coverage of the nebula, information on the velocity components is found in several radial velocity profiles in neighboring positions, facilitating their identification and decomposition.

Calibrating the fluxes may be done only indirectly, generally with HII regions for which absolute photometry exists. For N119 we have used the flux measured by Caplan & Deharveng (1985) in the central part of N119.

3. MAIN CHARACTERISTICS AND LOCAL ENVIRONMENT OF THE NEBULA N 119

3.1. *Ionized gas morphology*

The HII region N 119 (Henize 1956) or, following the new IAU nomenclature, B051842-6918 consists of three nebulae DEM L132a,b, DEM L123 and DEM L130 according to the DEM catalogue (Davies, Elliott, & Meaburn 1976). Hereafter we will designate all these nebulae as N 119 following the usual LMC denomination. N 119 forms a peculiar, intricate nebula. Although N 119 is smaller (131 $\times$ 175 pc, using 50 kpc for the LMC distance, and including ~80 pc

Fig. 2. Some of the [OIII] velocity channels in N 119. The upper channels show the bubble DEM L132b; the middle channels show the bubbles DEM L132a and DEM L123 and the lower channels show the WR bubble.

of filamentary extensions) than the 30 Doradus Nebula, it is remarkable for its peculiar spiral shape.

In Figure 1 the conspicuous morphology of N 119 can be appreciated in the [OIII] and Hα monochromatic images, extracted from our [OIII] and Hα FP cubes in the way discussed in § 2.

We can see a bright, elongated, central region (hereafter called "strong central emission", see Figure 1), with large and bright filamentary arcs on each extremity (hereafter called the NE and SW arcs, respectively). These arcs present ramifications formed of weaker filaments. The NE arc is 15′ long, and looks like a wavy filament. On the other hand, the

SW arc has a more rounded structure: to the west, a bright and broad arc can be seen, whereas to the east a faint filament seems to close the structure (a and b in Figure 1). An inspection of Figure 1 also reveals that N 119 is constituted by two sets of filaments which are clearly differentiated by their brightness: (1) a bright "S-shaped main structure" which includes the "strong central emission" and the arcs and (2) a series of faint filaments which seem to form four bubble-like structures. Figures 1 and 2 show the locations of these bubbles (DEM L132a, DEM L132b, DEM L123 and WR nebula) which are kinematically identified in § 4.
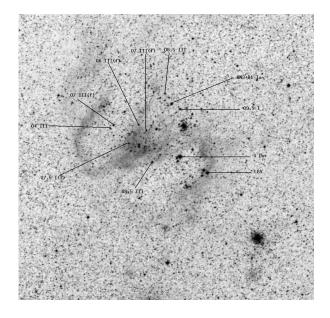
Fig. 3. $18' \times 18'$ DSS image of N 119 showing the positions of the most luminous stars.

The thermal radio continuum source MC30 (Mc Gee, Brooks, & Batchelor 1972) is associated with the optical nebula N 119.

3.2. *Stellar content*

The sole stellar association inside N 119 is LH41, which is an OB association with 52 members brighter than 14 mag (Lucke & Hodge 1970), spreading over $7' \times 4'$. Most of the stars of LH41 are located in the direction of the strong central emission; however, the more massive stars are located outside this emission (see Figure 3).

Among the massive stars, Br21 (Sk$-69°95$, HDE269333 or R87) is a Wolf-Rayet (WR) star of spectral type WN3+B1Ia (Walborn 1977; Conti & Massey 1989). Feast, Thackeray, & Wesselink (1960) have measured a radial velocity of $+286$ km s^{-1} for this star; however these authors have attributed only a "c" quality to this determination (their quality grade notes decrease from "a" to "d"). As Figure 3 shows, this WR star is located inside the WR nebula.

In the case of the star Sk$-69°104$ (HDE269357), Massey, Waterhouse, & DeGioia-Eastwood (2000) have determined a spectral type of O7III(f) and Ardeberg et al. (1972) have measured a stellar radial velocity of $+268$ km s^{-1} (based only upon one spectrum). As Figure 2 shows, this massive star and the star LH $41 - 32$ of O4III spectral type (Massey et al. 2000), are located inside the 132b Bubble.

The two more luminous stars to the south are of the SDor-type. The first one is SDor itself

(Sk$-69°94$, HD35343 or R88); the position of this star in the HR diagram is close to that of P-Cygni. Stothers & Chin (1996) have carried out a spectral analysis of SDor and determined a stellar mass of 23 $M_\odot$. Wesselink (1956) has measured a mean emission-line velocity of $+295$ km s^{-1} and, from absorption lines, $+213$ km s^{-1}. Van Genderen, Sterken, & de Groot (1997) have determined, from its light curves, that the temperature of SDor is fluctuating from 9000 K to 20 000 K. According to Szeifert et al. (1996) its mass-loss rate also varies from $\dot{M}_{LBV_{min}} = 10^{-6}$ $M_\odot$ yr^{-1} to $\dot{M}_{LBV_{max}} = 10^{-4} - 10^{-5}$ $M_\odot$ yr^{-1}. Recent observations (Massey 1999) report a FI-type spectrum, never observed so far for SDor. The other SDor-type star is Sk$-69°92$ (HDE269321 or R85, marked as LBV in Figure 3); Stahl et al. (1984) suggested that this star is either an SDor type F variable with a smaller amplitude than the classical cases, or that it is an SDor variable showing at present only small variations. In any case, this star is related to the SDor variables with $M_{BOL} = -9.7$, $T_{eff} = 13600$ K and $R = 135$ $R_\odot$. It has been classified as a B5I by Arp (1992).

3.3. *Gaseous Environment*

Israel et al. (1993) have detected three CO clouds towards N 119, two of them located along the northern arc (Figure 1). These authors have also measured a heliocentric radial velocity of $+279$ km s^{-1} for the more northern cloud, and of $+275$ km s^{-1} for the more southern cloud. The third cloud is located to the south of the strong central emission (Figure 1), but it is too faint for measuring any velocity. These data are collected in Table 1.

From HI observations with a resolution of $15'$ (218 pc), Rohlfs et al. (1984) have found two components along the line of sight of the northern nebulae (DEM L123 and DEM L132b), corresponding to the two components L ($\sim +275$ km s^{-1}) and D ($\sim +245$ km s^{-1}), and only one HI component along the line of sight of the strong central emission and southern arc (DEM L132a) corresponding to the D component mentioned before. From higher spatial resolution ($1'.5$) data Kim et al. (1999) have cataloged 2 giant shell candidates associated with DEM L123 (GS 51; $\alpha = 05^h16^m57^s, \delta = -69°09'45''$ J2000 and R=85 pc) and DEM L132b (GS54; $\alpha = 05^h18^m42^s, \delta = -69°10'00''$ J2000 and R=50 pc).

Figure 4 shows Spitzer observation at 8 microns (data available at NASA archive) superimposed on our Hα image. We can see that the photodissociation regions sourrounding the ionized gas match very well with the 132a bubble, the 132b bubble and the 123 nebula.

TABLE 1

RADIAL HELIOCENTRIC VELOCITIES (km s^{-1}) OF THE NEUTRAL
GAS SEEN ON THE LINE OF SIGHT OF N 119

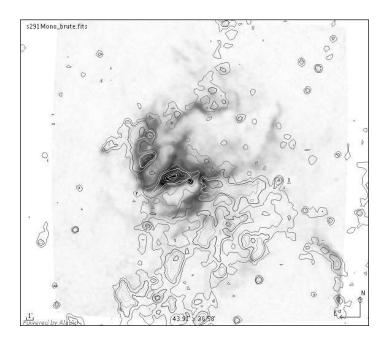|	CO Israel et al. (1993)	HI Rohlfs et al. (1984)	HI Kim et al. (1999)
DEM L123	279	246, 274	271
DEM L132b		244, 275	271
DEM L132a	275	266	
DEM L130	*	266	

*Detected cloud without velocity measurement.

Fig. 4. Contour map of Spitzer observation at 8 microns (data available at NASA archive) superposed on our Hα image. We can see that the photodissociation regions surrounding the ionized gas match very well with the 132a bubble, the 132b bubble and the 123 nebula.

The thermal radio continuum source MC30 (Mc Gee et al. 1972) is associated with the optical nebula N 119.

4. THE VELOCITY FIELD

Figure 2 presents the [OIII] FP velocity channels which show some emission separated by 7 km s^{-1}. In this figure it is seen that in addition to the strong central emission and arcs, which are quite well delineated, the nebula contains four fainter bubble-like nebulosities marked as bubbles 132a, 132b, WR nebula and DEM L123.

In general, the Hα and [OIII] radial velocity profiles show a main velocity component detected over the whole nebulosity at an average heliocentric ve-

locity of $+279$ km s^{-1} and with FWHM of 20 km s^{-1} and 7 km s^{-1} for the Hα and [OIII] velocity profiles, respectively (this corresponds to component number 2 in Figure 5). In addition to this main velocity component, the radial velocity profiles show several other velocity components that are coincident with different morphological features and that make the radial velocity profiles appear complex. In Figure 5 we have plotted radial velocity profiles of the different features, showing that superimposed on the velocity field of the S-shaped central body, which is quite regular and has a single velocity profile that will be analyzed in § 4.3, there are bubbles presenting complex velocity profiles and suggesting the existence of violent motions inside them. The perturbed zones
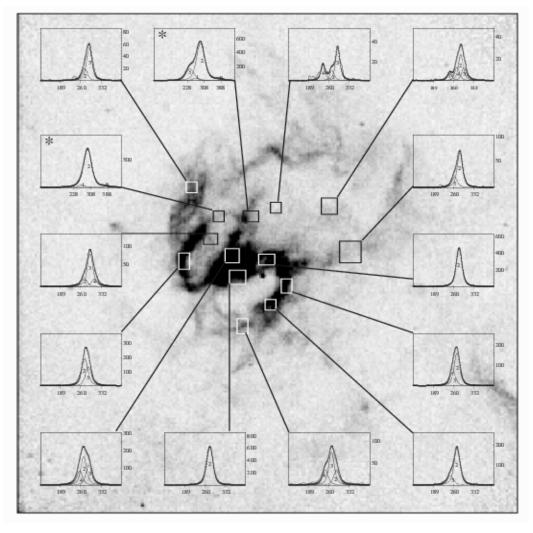
Fig. 5. Some examples of the Hα and [O III] radial velocity profiles of the different features of N 119 superimposed on an Hα image. The x-coordinate in the profiles gives the heliocentric radial velocity in km s^{-1} and the y-coordinate gives the intensity of the line in arbitrary units. Profiles marked with * are Hα radial velocity profiles. The velocity components marked as No. 0 and 1 in the Hα radial velocity profiles are night-sky lines. The velocity component marked as No. 2 is the main component found in the whole field (see text). The solid line corresponds to the sum of all the components. North is at the top and east is to the left.

are much fainter than the S-shaped central body and can be associated with some of the massive stars located within N 119, whose positions are also marked in Figure 3.

In the following section we will study the kinematics of these distinct bubbles, while § 4.3 is devoted to the study of the kinematics of the S-shaped central body.

4.1. Stellar Bubbles

In Figure 2 the bubbles 132a, 132b, WR nebula and DEM L123 mentioned before are shown. The stars associated with each nebula are listed in Table 2. Indeed, we have detected for the first time a

bubble around the WR star Br21, inside the N119 nebula, and we will show that it is a WR nebula given its computed age. The DEM L123 nebula does not seem to contain any interior exciting star.

On the other hand, the radial velocities in these bubbles are different from those of the neighboring gas, as can be seen in Figure 5, where typical velocity profiles of the bubbles and of the S-shaped nebular central body are also shown. This is not surprising because WR and Of stars have very strong winds that interact with the surrounding ISM, forming wind-blown bubbles (Weaver et al. 1977). In that way, we expect the existence of bubbles around very massive stars that undergo expansion motions,

TABLE 2

MAIN CHARACTERISTICS OF THE BUBBLES

Bubble name	Exciting star	α_{2000} of star	δ_{2000} of star	Spectral type	Radius (pc)	V_{min} km s^{-1}	V_{max} km s^{-1}	$S_{H\alpha}$ 10^{-5}erg cm^{-2} s^{-1} sr^{-1}
DEM L132b	Sk-69°104	$05^h18^m59.5^s$	$-69°12'55''$	O7III(f)	26	253	307	6.6
	LH 41-32	$05^h19^m1.9^s$	$-69°13'07''$	O4III				
WR	Br 21	$05^h18^m19.3^s$	$-69°11'41''$	WN3	26	230	298	4.9
DEM L123	SN?			SNR?	79	247	299	3.3
DEM L132a	S Dor	$05^h18^m14.4^s$	$-69°15'01''$	LBV	44	236	275	5.4
	Sk-69°92	$05^h17^m56.1^s$	$-69°16'03''$	LBV				

TABLE 3

PARAMETERS DERIVED FROM FABRY-PEROT OBSERVATIONS

Bubble name	V_{sys} km s^{-1}	V_{exp} km s^{-1}	n_e cm^{-3}	n_o cm^{-3}	t^+ 10^5 yr	L 10^{36} erg s^{-1}	L_{mec}* 10^{36} erg s^{-1}
DEM L132b	285	27	19	2.6	6	12	13
WR nebula	285	34	20	1.7	5	15	100
DEM L123	279	26	8	1.2	18	44	–
DEM L132a	272	20	10	2.5	13	13	0.2–2

$^+$Dynamic timescale.

*Mechanical luminosity of the stellar wind.

whose signature is the presence of splitting of the velocity profiles at the center of the bubbles (near the position of the exciting star), while at the bubble boundaries the velocity profiles are single. We have found this kinematic evidence for the bubbles shown in Figure 5. In Table 2 we report the main measured parameters of the bubbles such as: name of the bubble, exciting star denomination, spectral type of the exciting star, linear radius, R, extreme velocity components, V_{min} and V_{max}, and Hα surface brightness, $S_{H\alpha}$.

On the basis of Hα and Hβ photometry, the color excess of the nebula N 119 has been deduced by Caplan & Deharveng (1985, 1986) as $E_{(B-V)} = 0.15$. The Lyman flux measured by Smith, Cornett, & Hill (1987) from UV observations of the OB association LH41 (1.05×10^{51} photons per second) is larger than the one derived from the 6-cm observations of McGee et al. (1972) (2.4×10^{50} photons per second) and the one derived from our Hα flux (1.3×10^{50} photons per second), implying that the UV flux of the interior massive stars is more than enough to photoionize the nebula (see § 4)

The Lyman flux for the 132a bubble obtained from our Hα flux is 7.1×10^{49} photons per second; this value corresponds to an O3I star (Martins, Schaerer, & Hillier 2005) or an O3V or O4III (Vacca, Garmany, & Shull 1996). However no OB star has been identified interior to the bubble 132a. The low temperature of the SDor variable stars indicates that they cannot contribute to the yield of the Lyman photon flux, but it is possible that this bubble has been driven by the wind of the earlier phase of SDor.

On the other hand, from the measured parameters listed in Table 2 we can deduce several physical properties of the bubbles by applying the models of stellar wind-driven bubbles developed by Weaver et al. (1977).

Table 3 lists, in Column 1, the bubble name. Column 2 gives the systemic velocity of the ionized gas, Column 3 gives the expansion velocity, Column 4 shows the rms electron density, Column 5 the pre-shock density and Column 6 the dynamical time scale. In Column 7 the wind luminosity required to drive the measured bubble expansion is obtained; in Column 8 an estimate of the available mechanical luminosity of the winds is given.

The systemic velocities of the ionized gas were obtainded from the average heliocentric velocities of the total Hα emission. The expansion velocity, was

obtained as: $V_{\mathrm{exp}} = (V_{\mathrm{max}} - V_{min})/2$. The rms electron density, n_e, has been evaluated by assuming a shell thickness $\Delta R = (R/3(1 + \frac{V_S^2}{C^2}))$ (Weaver et al. 1977) where V_S is the shock velocity in km s^{-1}. The pre-shock density, n_o, has been obtained from n_e and V_{exp} by assuming an isothermal shock: $n_o = (C_S/V_S)^2 n_e$, where C_S is the sound speed in the ambient medium and V_S is the shock velocity. We take $C_S = 10$ km s^{-1} for an ambient medium at 10^4 K and $V_S = V_{\mathrm{exp}}$. The dynamical time scale, t, is obtained as $0.59 R/V_S$ (Weaver et al. 1977), where t is in units of 10^6 years, R in pc and V_S in km s^{-1}. The required wind luminosity in order to drive the measured bubble expansion is obtained as: $L = 3.35 \times 10^{-7} R^2 n_o V_S^3$, where L is given in units of 10^{36} ergs s^{-1}, R in pc, n_o in cm^{-3} and V_S in km s^{-1}. An estimate of the available mechanical luminosity of the winds, $L_{\mathrm{mec}} = 0.5\, \dot{M}\, V_w^2$ in units of 10^{36} erg s^{-1} is obtained by taking the terminal velocity of stellar wind from Walborn et al. (1995) and Koesterke et al. (1991). The mass-loss rate comes from the Conti & Underhill (1988) calibrations.

In the case of bubble DEM L132b (associated with the O7 and O4 supergiant stars) the value of the mechanical luminosity of the stellar wind (L_{mec}) is comparable to the required wind power (L) to drive the bubble. Thus, the expansion of this bubble is fully accounted for by the interior O supergiant stars.

In the case of the WR nebula, the available mechanical luminosity of a WR star of the same spectral type is much larger than the wind luminosity required to drive the WR nebula. Thus, the WR star could account amply for producing the expansion motion. Furthermore, from Maeders's (1996) models, the lifespan of the WR phase for a star with an initial mass of 55 $M_{\odot}$ (the typical initial mass of a WN3 star) is 5×10^5 yrs. Consequently, as the dynamic timescale matches well with the duration of the WR phase, it is proposed that this bubble was formed by the action of the stellar wind of the central WR star.

4.2. The supernova remnant candidate DEM L123

Bubble DEM L123, also marked in Figure 2, is located to the NW of the S-shaped central body of N 119. In addition, this optical ring coincides with the position of a HI giant shell cataloged by Kim et al. (1999) but, unfortunately, these authors do not give the dimensions of the HI shell.

In Figure 5, the [OIII] velocity profiles at several positions in ubble DEM L123 are shown. From this figure it can be appreciated that bubble DEM L123 undergoes an expansion motion because the

kinematic field displays simple and narrow velocity profiles in the outer regions surrounding a central zone of more complex [OIII] velocity profiles.

The Hα and [OIII] radial velocity profiles show a main velocity component detected over the whole nebulosity at an average heliocentric velocity of $+279$ km s^{-1} and with a FWHM of 20 km s^{-1} and 7 km s^{-1} for the Hα and [OIII] velocity profiles, respectively (this corresponds to component number 2 in Figure 5). On the other hand, extreme velocities are measured in the [OIII] line near the geometrical center of this nebula. The most redshifted velocity value is $+299$ km s^{-1} (with S/N=6) and the most blueshifted one is $+247$ km s^{-1} (with S/N=4).

The measured parameters for this nebula are also quoted in Table 2 while the derived physical properties are reported in Table 3. We see that applying stellar wind models to the energetic input in DEM L123 would thus require at least the presence of 44 O6 supergiant stars, while there are no blue stars detected inside this nebula. At most, a group of faint stars is located at the eastern periphery of this bubble; these stars show UV emission (Parker et al. 1999) and may contribute to partially ionize the bubble but no evidence of strong stellar winds is found. On the other hand, if we assume that this nebula is a supernova remnant (SNR) then, by applying the results of Chevalier (1974) for a SNR in the radiative phase in the same way as for N103 (Ambrocio-Cruz et al. 1997), we obtain 10^{52} erg as the initial energy, E_o, required to explain the bubble energetics. The assumption of an energy input by a supernova explosion is not plausible, since the typical value of such an event is about 10^{51} erg. However, it should be noticed that other similar large diameter bubbles have been proposed to be candidates to old SNRs in the LMC, as is the case of the bubble N186E (Rosado et al. 1990), though for that case, the energetics can be fully accounted for by a typical SN explosion. A hypernova explosion could account for this bubble (Lozinskaya & Moiseev 2007), but no other signs of this kind of event, such as non-thermal radio emission, have been detected (Richer et al. 2001).

4.3. The velocity field of the S-shaped central body

As mentioned before, in addition to the main component present over the entire field at a heliocentric velocity of about $+279$ km s^{-1}, which we take as the nebular systemic velocity, the Hα and [OIII] velocity profiles of the bubbles present splitting and broadening in several places. Furthermore, there is a difference in intensities between the emission of the S-shaped central body, which has a S/N

ratio of 330, and the emission of the fainter regions, where the S/N~4.

Figure 5 also shows the velocity profiles. The range of the velocity values of the main component in the field is 277–281 km s^{-1}. In addition to this component, other redshifted ($\sim$+395 km s^{-1}) and blueshifted velocity components ($\sim$+255 km s^{-1})(profiles 3 and 4 of Figure 5) are detected in the northern and southern regions of the S-shaped central body, respectively.

In the next section, a discussion will be presented trying to interpret the kinematic field and morphology of the S-shaped central body of N 119.

5. DISCUSSION OF THE ORIGIN OF THE NEBULAE

The conspicuous shape of the nebular complex N 119 can be interpreted as a result of the superposition of several types of bubbles formed by different mechanisms taking place in this complex. The bubbles could be naturally formed by the interaction of the strong stellar winds of the massive interior stars with the surrounding ISM. We have estimated the physical properties of these bubbles and shown that two of them can be formed by the Of and WR stellar winds (DEM L132b Bubble and WR nebula, respectively). The energy requirements of one of the bubbles (DEM L123) imply the existence of several interior OB stars that have not been detected yet. The possible detection of diffuse X-ray emission in N 119 by Chu & Mac Low (1990) is a marginal evidence for the possibility that this nebula is an old SNR, or possibly the remnant of a hypernova explosion. However, no other signatures of the presence of a SNR, such as non-thermal radio emission or high [SII]/Hα line-ratios, have been found. Consequently, the nature of Bubble DEM L123 is still uncertain.

The Lyman flux measured by Smith et al. (1987) from UV observations of the OB association LH41 (1.05×10^{51} ph s^{-1}) is larger than the one derived from the 6 cm observations of McGee et al. (1972) (2.4×10^{50} ph s^{-1}) and the one derived from our Hα flux (1.3×10^{50} ph s^{-1}). So we have here a case of a density-bounded nebula, at least in some directions.

6. CONCLUSIONS

N119 seems to contain three expanding bubble-shaped nebulae formed by the action of the stellar winds from Wolf-Rayet (WR bubble) and O stars (DEM L132b). Indeed, we have detected for the first time a bubble around the WR star Br 21 inside the N119 nebula, and we suggest that it is a WR nebula. The nature of the largest nebula (DEM L123) is still uncertain; we suggest that it is a posible remnant of a hypernova explosion.

From observations at 8 microns the photodissociation regions surrounding the ionized gas match very well with the 132a bubble,the 132b bubble and the 123 nebula.

According to these results, the spiral shape of N119 could be due to the interaction of the detected bubbles. In favor of this scenario is the increased brightness of the zone. However, some of the bubbles have different systemic velocities and they may not coincide spatially. The spiral shape of N119 can be only apparent or can be due to the interaction of several bubbles at different systemic velocities.

According to these results, we think that the spiral shape of N119 could be produced by the perforation of an original molecular cloud (now the central body) by the ionization, winds and possible hypernova explosion of some of the massive interior stars. Another possibility is that the shape of N119 is due to the interaction of the several expanding bubbles that we have detected; this however, does not explain the minimum complexity of the velocity profiles in the main body (pressumably, the zone of interaction). In adition, the different systemic velocities of two of the four bubbles can be seen as a projection effect, and consequently, the hypothesis of a true collision between the different nebulae weakens.

REFERENCES

Ambrocio-Cruz, P., Laval, A., Marcelin, M., & Amram, P. 1997, A&A, 319, 973

Ardeberg, A., Brunet, J. P., Maurice, E., & Prévot, L. 1972, A&AS, 6, 249

Arp, H. 1992, MNRAS, 258, 800

Caplan, J., & Deharveng, L. 1985, A&AS, 62, 63

_____. 1986, A&A, 155, 297

Chevalier, R. A. 1974, ApJ, 188, 501

Chu, Y.-H., & Mac Low, M. 1990, ApJ, 365, 510

Conti, P. S., & Massey, P. 1989, ApJ, 337, 251

Conti, P. S., & Underhill, A. B. (ed.) 1988, O Stars and Wolf-Rayet Stars (NASA SP-497) (Washington: NASA)

Davies, R. D., Elliott, K. M., & Meaburn, J. 1976, MmRAS, 81, 89

Feast, M. W., Thackeray, A. D., & Wesselink, A. J. 1960, MNRAS, 121, 337

Georgelin, Y. M., Georgelin, Y. P., Laval, A., Monnet, G., & Rosado, M. 1983, A&AS, 54, 459

Henize, K. G. 1956, ApJS, 2, 315

Israel, F. P., et al. 1993, A&A, 276, 25

Kim, S., Dopita, M. A., Staveley-Smith, L., & Bessell, M. 1999, AJ, 118, 2797

Kim, S., Staveley-Smith, L., Dopita, M. A., Freeman, K., Saulte, J., Kesteven, M., & McConnell, D. 1998, ApJ, 503, 674

Koesterke, L., Hamann, W.-R., Wessolowski, U., & Schmutz, W. 1991, A&A, 248, 166

Le Coarer, E., Rosado, M., Georgelin, Y. P., Viale, A., & Goldes, G. 1993, A&A, 280, 365

Lozinskaya, T. A., & Moiseev, A. V. 2007, MNRAS, 381, 26

Lucke, P. B., & Hodge, P. W. 1970, AJ, 75, 171

Maeder, A. 1996, Proc. 33rd Liège Intern. Astroph. Colloq., Wolf-Rayet Stars in the Framework of Stellar Evolution, ed. J. M. Vreux, et al. (Liège: Institut d'Astrophysique), 39

Martins, F., Schaerer, D., & Hillier, D. J. 2005, A&A, 436, 1049

Massey, P. 1999, IAU Circ., 7290, 1

Massey, P., Waterhouse, E., & DeGioia-Eastwood, K. 2000, AJ, 119, 2214

McGee, R. X., Brooks, J. W., & Batchelor, R. A. 1972, Aust. J. Phys., 25, 581

Meaburn, J., McGee, R. X., & Newton, L. M. 1984, MNRAS, 206, 705

Parker, J. W., et al. 1999, IAU Symp. 190, New Views of the Magellanic Clouds, ed. Y.-H. Chu, N. Suntzeff, J. Hesser, & D. Bohlender (San Francisco: ASP), 237

Richer, M. G., et al. 2001, A&A, 370, 34

Rohlfs, K., Kreitschmann, J., Siegman, B. C., & Feitzinger, J. V. 1984, A&A, 137, 343

Rosado, M. 1986, A&A, 160, 211

Rosado, M., et al. 1990, A&A, 238, 315

Smith, A. M., Cornett, R. H., & Hill, R. S. 1987, ApJ, 320, 609

Stahl, O., Wolf, B., Leitherer, C., Zickgraf, F., Krautter, J., & de Groot, M. 1984, A&A, 140, 459

Stothers, R. B., & Chin, C. 1996, ApJ, 468, 842

Szeifert, T., Humphreys, R., Davidson, K., Jones, T., Stahl, O., Wolf, B., & Zickgraf, F. 1996, A&A, 314, 131

Vacca, W. D., Garmany, C. D., & Shull, J. M. 1996, ApJ, 460, 914

Van Genderen, A. M., Sterken, C., & de Groot, M. 1997, A&A, 318, 81

Walborn, N. R. 1977, ApJ, 215, 53

Walborn, N. R., Lennon, D. J., Haser, S. M., Kudritzki, R., & Voels, S. 1995, PASP, 107, 104

Weaver, R., Mc Cray, R., Castor, J., Shapiro, P., & Moore, R. 1977, ApJ, 218, 377

Wesselink, A. J. 1956, MNRAS, 116, 3

P. Ambrocio-Cruz: Instituto de Astronomía, Universidad Nacional Autónoma de México, Apdo. 70-264, 04510, México, D.F., Mexico (patricia@astroscu.unam.mx) and Dpto. de Física, Universidad Iberoamericana, Prol. Paseo de la Reforma 880, Lomas de Santa Fe, 01210, México, D.F., Mexico.

P. Amram, A. Laval, and D. Russeil: LAM, Observatoire de Marseille, 2, Place Le Verrier, 13248 Marseille CEDEX 4, France (delphine.russeil@oamp.fr).

E. Lecoarer: Laboratoire d'Astrophysique de Grenoble, B.P. 53 Grenoble CEDEX 9, France (etienne.lecoarer@obs.ujf-grenoble.fr).

M. Rosado: Instituto de Astronomía, Universidad Nacional Autónoma de México, Apdo. 70-264, 04510, México, D.F., Mexico (margarit@astroscu.unam.mx).